Interactions between SF_4 and Fluoride: A Crystallographic Study of Solvolysis Products of SF_4·Nitrogen Base Adducts by HF

James T. Goettel,[a] Nathan Kostiuk,[a] Michael Gerken[a, *]

Contribution from the Department of Chemistry and Biochemistry, University of Lethbridge, Lethbridge, Alberta T1K 3M4, Canada and the Canadian Centre for Research in Advanced Fluorine Technologies, University of Lethbridge, Lethbridge, Alberta T1K 3M4, Canada

[*] Corresponding author. Tel.: +1-403-329-2173; fax: +1-403-329-2057. *e-mail address*: michael.gerken@uleth.ca.

[a] University of Lethbridge

Abstract

Adducts between SF_4 and a nitrogen base are easily solvolysed by HF, yielding the protonated nitrogen base and fluoride. Salts resulting from the solvolysis of $SF_4{\cdot}NC_5H_5$, $SF_4{\cdot}NC_5H_4(CH_3)$, $SF_4{\cdot}NC_5H_3(CH_3)_2$, and $SF_4{\cdot}NC_5H_4N(CH_3)_2$ have been studied by Raman spectroscopy and X-ray crystallography. Crystal structures were obtained for pyridinium salts: $[HNC_5H_5^+]F^-{\cdot}SF_4$, $[HNC_5H_5^+]F^-[HF]{\cdot}2SF_4$; the 4-methylpyridinium salt: $[HNC_5H_4(CH_3)^+]F^-{\cdot}SF_4$; 2,6-methylpyridinium salt: $[HNC_5H_3(CH_3)_2^+]_2[SF_5^-]F^-{\cdot}SF_4$; and 4-dimethylaminopyridinium salts: $[HNC_5H_4N(CH_3)_2^+]_2[SF_5^-]F^-{\cdot}CH_2Cl_2$, $[NC_5H_4N(CH_3)_2^+][HF_2^-]{\cdot}2SF_4$. In addition, the structure of $[HNC_5H_4(CH_3)^+][HF_2^-]$ was obtained. 4,4'-bipyridyl reacts with SF_4 and one or two equivalents of HF to give the 4,4'-bipyridinium salts $[NH_4C_5{-}C_5H_4NH^+]F^-{\cdot}2SF_4$ and $[HNH_4C_5{-}C_5H_4NH^{2+}]2F^-{\cdot}4SF_4$, respectively. These structures exhibit a surprising range of bonding modalities and provide an extensive view of SF_4 and its contacts with Lewis-basic groups in the solid state. The interactions range from the strong $F_4S{-}F^-$ bond in the previously observed SF_5^- anion to weak $F_4S{-}{-}{-}F^-$, $F_4S(---F^-)_2$ and $F_4S(---FHF^-)_2$ dative bonds.

Introduction

Sulfur tetrafluoride is a binary covalent fluoride that is of fundamental interest to inorganic chemistry and that has applications in organic as well as inorganic chemistry as a deoxofluorinating reagent.[1,2] Low-temperature Raman spectroscopic and X-ray crystallographic studies showed that SF_4 is Lewis acidic toward organic bases, forming 1:1 adducts with the nitrogen-bases, trimethylamine,[3] pyridine, 4-methylpyridine, 2,6-dimethylpyridine, and 4-dimethylaminopyridine.[4] These adducts are stable below −40 °C under dynamic vacuum and exhibit N---S(IV) dative bonds ranging from 2.141(2) to 2.514(2) Å. Sulfur tetrafluoride can also act as a Lewis acid towards strong fluoride ion donors forming the SF_5^- anion. For example, SF_4 reacts with anhydrous $[N(CH_3)_4]F$, a naked fluoride source, to form the $[N(CH_3)_4^+][SF_5^-]$ salt, which was first reported in 1963.[5] The Rb^+, Cs^+, and $[(CH_3)_2N]_2S^+$ salts of the SF_5^- anion have since been prepared and characterized by vibrational spectroscopy.[6-9] Only four crystal structures have been reported containing the SF_5^- anion: $Rb^+[SF_5^-]$,[6] $Cs^+{}_6[SF_5^-]_4[HF_2^-]_2$,[6] $[Cs(18\text{-crown-}6)_2^+][SF_5^-]$,[10] and $[HNC_5H_3(CH_3)_2^+]_2F^-[SF_5^-]\cdot 4SF_4$.[11] The latter SF_5^- salt was obtained by reaction of the $SF_4\cdot$2,6-$NC_5H_3(CH_3)_2$ adduct with HF and crystallization below −90 °C. This reaction documents the facile solvolysis of SF_4 - nitrogen-base adducts by HF. The current study reports the systematic investigation of such solvolysis reactions of SF_4 adducts and the structures of their products.

Results and Discussion

Synthesis and Properties

As expected, SF_4·N-base adducts were found to be very sensitive towards traces of moisture. Large needle-like crystals of the composition $[HNC_5H_5^+]F^-\cdot SF_4$ were obtained by

recrystallization of the $SF_4 \cdot NC_5H_5$ adduct in toluene containing traces of moisture. Trace amounts of water hydrolyzed SF_4 producing HF (Eq. 1), which then solvolysed the $SF_4 \bullet NC_5H_5$ adduct, resulting in protonation of the base and formation of fluoride (Eq. 2).

$$SF_4 + H_2O \rightarrow SOF_2 + 2\ HF \quad (1)$$

$$SF_4 \cdot NC_5H_5 + HF \rightarrow [HNC_5H_5^+]F^- \cdot SF_4 \quad (2)$$

In attempts to reproduce the solvolysis quantitatively, reactions of pyridine with excess aHF and SF_4 were carried out, but gave a multitude of products which were difficult to isolate, presumably containing a range of polyhydrogenfluoride anions. The products, obtained after removal of volatiles at low temperature, often did not contain SF_4 as shown by Raman spectroscopy. Attempts at measuring equimolar amounts of HF to pyridine, while excluding H_2O, proved to be exceedingly difficult. The use of stoichiometric amounts of water as a reagent, added with the aid of a microsyringe, to generate HF *in situ* via hydrolysis of excess SF_4 (Eq. 1), was shown to be a successful preparative route to systematically study the solvolysis products of SF_4·N-base adducts. The by-product, thionyl fluoride, did not interfere with the reaction chemistry and could be removed under dynamic vacuum at low temperature. Attempts to obtain crystals of $[HNC_5H_5^+]F^- \cdot SF_4$, however, were unsuccessful when SF_4 was used as a solvent, in place of toluene. Instead, $[HNC_5H_5^+][HF_2^-] \bullet 2SF_4$ crystallized under these conditions (Eq. 3), even when a 1:1 ratio of HF to pyridine was used.

$$SF_4 \cdot NC_5H_5 + 2HF + SF_4 \rightarrow [HNC_5H_5^+][HF_2^-] \cdot 2SF_4 \quad (3)$$

The reaction of a 2:1 mixture of 4-methylpyridine and water in excess SF_4, corresponding to a 1:1 ratio of $SF_4 \cdot 4\text{-}NC_5H_4(CH_3)$ to HF, at room temperature yielded $[HNC_5H_4(CH_3)^+]F^- \cdot SF_4$ (Eq. 4) in admixture with unreacted $SF_4 \cdot 4\text{-}NC_5H_4(CH_3)$. Increasing the HF to adduct ratio to 1.5:1 resulted in significant reduction of $SF_4 \cdot 4\text{-}NC_5H_4(CH_3)$. The $[HNC_5H_4(CH_3)^+]F^- \cdot SF_4$ salt could be isolated with a small $SF_4 \cdot 4\text{-}NC_5H_4(CH_3)$ impurity after removal of excess SF_4 and SOF_2 under dynamic vacuum at low temperature.

$$SF_4 \cdot 4\text{-}NC_5H_4(CH_3) + HF \rightarrow [HNC_5H_4(CH_3)^+]F^- \cdot SF_4 \quad (4)$$

The reaction of $2,6\text{-}NC_5H_3(CH_3)_2$ in excess SF_4 with an equimolar amount of HF was previously shown to yield $[HNC_5H_3(CH_3)_2^+]_2F^-[SF_5^-] \cdot 4SF_4$ (Eq. 5) when volatiles were removed at −90 °C.[11] Under these conditions, crystals with a different habit were observed in addition to those of $[HNC_5H_3(CH_3)_2^+]_2F^-[SF_5^-] \cdot 4SF_4$. These new crystals were shown to be those of $[HNC_5H_3(CH_3)_2^+]_2[SF_5^-]F^- \cdot SF_4$, which contains three SF_4 molecules less per formula unit than the previous structure. As previously reported, $[HNC_5H_3(CH_3)_2^+]_2F^-[SF_5^-] \cdot 4SF_4$ readily loses SF_4,[11] yielding $[HNC_5H_3(CH_3)_2^+]_2[SF_5^-]F^- \cdot SF_4$ under dynamic vacuum at −70 °C as observed by Raman spectroscopy (Eq. 6).

$$SF_4 \cdot 2,6\text{-}NC_5H_3(CH_3)_2 + HF \rightarrow [HNC_5H_3(CH_3)_2^+]_2F^-[SF_5^-] \cdot 4SF_4 \quad (5)$$

$$[HNC_5H_3(CH_3)_2^+]_2F^-[SF_5^-] \cdot 4SF_4 \rightarrow [HNC_5H_3(CH_3)_2^+]_2[SF_5^-]F^- \cdot SF_4 + 3SF_4 \quad (6)$$

Similar to the $SF_4{\cdot}NC_5H_5$ adduct, $SF_4{\cdot}NC_5H_4N(CH_3)_2$ was solvolysed using equimolar amounts of HF in SF_4 solvent to form crystals of the bifluoride salt $[HNC_5H_4N(CH_3)_2^+][HF_2^-]{\cdot}2SF_4$ (Eq. 7).

$$SF_4{\cdot}NC_5H_4N(CH_3)_2 + 2HF + SF_4 \rightarrow [HNC_5H_4N(CH_3)_2^+][HF_2^-]{\cdot}2SF_4 \quad (7)$$

Since the $SF_4{\cdot}NC_5H_4N(CH_3)_2$ adduct is essentially insoluble in excess SF_4, CH_2Cl_2 was added to dissolve the adduct. Removal of volatiles at −60 °C led to the formation of fine crystalline needles of the composition $[HNC_5H_4N(CH_3)_2^+]_2[SF_5^-]F^-{\cdot}CH_2Cl_2$ as determined by Raman spectroscopy and X-ray crystallography. Apparently, traces of water hydrolyzed half of the SF_4 molecules forming HF and SOF_2, yielding a salt that contained 1:2 ratio of SF_4 to dimethylaminopyridinium (Eq 8).

$$2SF_4{\cdot}NC_5H_4N(CH_3)_2 + H_2O + CH_2Cl_2 \rightarrow [HNC_5H_4N(CH_3)_2^+]_2[SF_5^-]F^-{\cdot}CH_2Cl_2 + SOF_2 \quad (8)$$

The solubility of 4,4'-bipyridyl in neat SF_4 is very low. It can be greatly increased by singly protonating 4,4'-bipyridyl in neat SF_4 using HF. Varying the molar ratio of HF to 4,4'bipyridyl yielded different products. A 1:1 ratio of HF to 4,4-bipyridyl (resulting from a 1-to-2 mixture of H_2O to 4,4'-bipyridyl) in excess SF_4 produced the singly protonated bipyridinium salt $[HNH_4C_5{-}C_5H_4N^+]F^-{\cdot}2SF_4$ (Eq. 9), while a 2:1 mixture of HF to 4,4-bipyridyl (1:1 ratio of H_2O to 4,4'-bipyridyl) in excess SF_4 yielded the doubly protonated bipyridinium salt $[HNH_4C_5{-}C_5H_4NH^{2+}]2F^-{\cdot}4SF_4$ (Eq. 10).

$$F_4S{\cdot}NH_4C_5{-}C_5H_4N{\cdot}SF_4 + HF + 2SF_4 \rightarrow [HNH_4C_5{-}C_5H_4N^+]F^-{\cdot}2SF_4 \quad (9)$$

$$F_4S{\cdot}NH_4C_5{-}C_5H_4N{\cdot}SF_4 + 2HF + 4SF_4 \rightarrow [HNH_4C_5{-}C_5H_4NH^{2+}]2F^-{\cdot}4SF_4 \quad (10)$$

All solid samples containing SF_4 are stable only at low temperature, since they readily lose SF_4 upon warming. Therefore, all samples had to be manipulated at low temperature. Generally, when stoichiometric amounts of reagents were used, the yields were quantitative based on Raman spectroscopy, except in the case of $[HNC_5H_4(CH_3)^+]F^-{\cdot}SF_4$, where an excess of HF was needed. Reactions with a deficiency of HF yielded the previously characterized SF_4·N-adducts. An excessive amount of SF_4 did not result in precipitation or crystallization of the product. It is imperative to remove the volatiles at low-temperatures, or the adducted SF_4 will be lost.

X-ray Crystallography

Selected crystallographic data the X-ray crystal structures are listed in Table 1, whereas selected bond lengths and angles are given in Table 2.

Pyridine-HF-SF_4 System. The $[HNC_5H_5^+]F^-{\cdot}SF_4$ salt crystallizes in the orthorhombic space group, *Pbca*. The structure consists of infinite chains along the *c*-axis with SF_4 molecules linked by fluoride anions, forming S---F---S bridges (Figure 1).

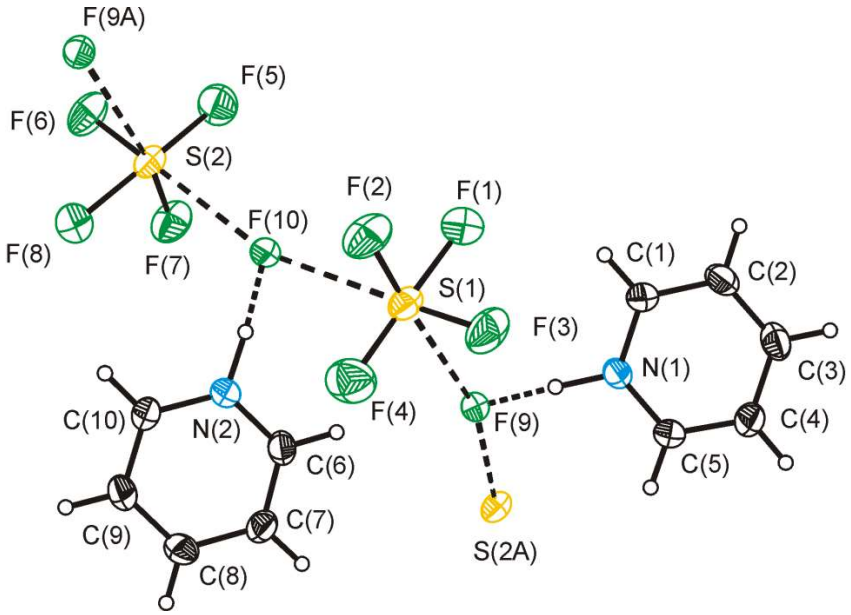

Figure 1. Thermal ellipsoid plot of a chain in the crystal structure of $[HNC_5H_5^+]F^- \cdot SF_4$ with thermal ellipsoids at 50% probability.

Table 1. Crystallographic Data for $[HNC_5H_5^+]F^-\cdot SF_4$, $[HNC_5H_5^+][HF_2^-]\cdot 2SF_4$, $[HNC_5H_4(CH_3)^+]F^-\cdot SF_4$, $[HNC_5H_4(CH_3)^+][HF_2^-]$, $[HNC_5H_3(CH_3)_2^+]_2[SF_5^-]F^-\cdot SF_4$, $[HNC_5H_4N(CH_3)_2^+][HF_2^-]\cdot 2SF_4$, $[HNC_5H_4N(CH_3)_2^+]_2[SF_5^-]F^-\cdot CH_2Cl_2$, $[HNH_4C_5{-}C_5H_4NH^{2+}]2F^-\cdot 2SF_4$, and $[HNH_4C_5{-}C_5H_4N^+]F^-\cdot 4SF_4$.

Compound	$[HNC_5H_5^+]F^-\cdot SF_4$	$[HNC_5H_5^+][HF_2^-]\cdot 2SF_4$	$[HNC_5H_4(CH_3)^+]F^-\cdot SF_4$	$[HNC_5H_4(CH_3)^+][HF_2^-]$	$[HNC_5H_3(CH_3)_2^+]_2[SF_5^-]F^-\cdot SF_4$
Empirical Formula	$C_5H_6F_5NS$	$C_5H_7F_{10}NS_2$	$C_6H_8F_5NS$	$C_6H_9F_2N$	$C_{14}H_{20}F_{10}N_2S_2$
Mass	207.17	335.24	221.20	133.14	470.44
Crystal system	orthorhombic	Monoclinic	triclinic	Orthorhombic	monoclinic
Space group	*Pbca*	*C2/m*	$P\bar{1}$	*Pnma*	$P2_1/n$
a [Å]	13.919(4)	16.366(11)	7.261(16)	19.22(4)	7.8081(6)
b [Å]	13.681(4)	8.794(6)	8.419(18)	7.741(16)	18.207(4)
c [Å]	17.101(4)	8.842(6)	8.705(19)	4.74(1)	14.352(3)
α	90	90	61.90(2)	90	90
β	90	116.566(7)	82.15(2)	90	99.917(2)
γ	90	90	75.28(2)	90	90
V [Å^3]	3256.4(15)	1138.1(13)	453.9(17)	705(2)	2009.9(7)
Z	16	4	2	4	4
Calcd density [g cm^{-3}]	1.690	1.956	1.618	1.254	1.555
T [°C]	−120	−120	−120	−120	−120
μ [mm^{-1}]	0.43	0.58	0.39	0.11	0.36
$R_1{}^a$	0.0298	0.0466	0.0295	0.0366	0.038
$wR_2{}^b$	0.0936	0.1089	0.0884	0.1148	0.111
CCDC number	1477908	1477906	1477909	1477907	1477905

Compound	$[HNC_5H_4N(CH_3)_2^+][HF_2^-]\cdot 2SF_4$	$[HNC_5H_4N(CH_3)_2^+]_2[SF_5^-]F^-\cdot CH_2Cl_2$	$[HNH_4C_5{-}C_5H_4N^+]F^-\cdot 2SF_4$	$[HNH_4C_5{-}C_5H_4NH^{2+}]2F^-\cdot 4SF_4$
Empirical Formula	$C_7H_{12}F_{10}N_2S_2$	$C_{15}H_{24}Cl_2F_6N_4S$	$C_{10}H_9F_9N_2S_2$	$C_{10}H_{10}F_{18}N_2S_4$
Mass	378.31	477.34	392.31	628.44
Crystal system	Monoclinic	Monoclinic	Orthorhombic	Tetragonal
Space group	$P2_1/c$	$P2_1/n$	$P2_12_12_1$	$P\bar{4}2_1c$
a [Å]	8.605(6)	7.001(5)	7.339(7)	16.530(13)
b [Å]	20.371(15)	14.351(10)	10.783(10)	16.530(13)
c [Å]	16.500(12)	21.647(15)	18.641(17)	8.322(6)
α	90	90	90	90
β	90.415(9)	96.742(8)	90	90
γ	90	90	90	90
V [Å^3]	2892(4)	2160(3)	1475(2)	2274(3)
Z	8	4	4	4
Calcd density [g cm^{-3}]	1.738	1.468	1.783	1.836
T [°C]	−120	−120	−120	−120
μ [mm^{-1}]	0.47	0.46	0.46	0.57
R_1[a]	0.0324	0.0690	0.0377	0.0324
wR_2[b]	0.0867	0.1721	0.1041	0.0882
CCDC number	1477911	1477910	1477904	1477903

[a] R_1 is defined as $\Sigma||F_o| - |F_c||/\Sigma|F_o|$ for $I > 2\sigma(I)$. [b] wR_2 is defined as $[\Sigma[w(F_o^2 - F_c^2)^2]/\Sigma w(F_o^2)^2]^{1/2}$ for $I > 2\sigma(I)$.

Table 2. Selected bond lengths (Å), contacts (Å) and angles (°) of the SF_4 moieties in the structures of $[HNC_5H_5^+]F^-\cdot SF_4$, $[HNC_5H_5^+][HF_2^-]\cdot 2SF_4$, $[HNC_5H_4(CH_3)^+]F^-\cdot SF_4$, $[HNC_5H_3(CH_3)_2^+]_2[SF_5^-]F^-\cdot SF_4$, $[HNC_5H_4N(CH_3)_2^+][HF_2^-]\cdot 2SF_4$, $[HNH_4C_5{-}C_5H_4NH^{2+}]2F^-\cdot 2SF_4$, and $[HNH_4C_5{-}C_5H_4N^+]F^-\cdot 4SF_4$.

	$[HNC_5H_5^+]F^-\cdot SF_4$	$[HNC_5H_5^+][HF_2^-]\cdot 2SF_4$	$[HNC_5H_4(CH_3)^+]F^-\cdot SF_4$	$[HNC_5H_3(CH_3)_2^+]_2[SF_5^-]F^-\cdot SF_4$
$S{-}F_{eq}$	1.5382(9), 1.5440(9)	1.535(2), 1.537(2)	1.543(4), 1.544(4)	1.5415(11), 1.5538(13)
$S{-}F_{ax}$	1.6622(11), 1.6680(11)	1.643(3), 1.670(3)	1.650(4), 1.652(4)	1.6557(12), 1.6736(12)
S---F	2.6826(9), 2.7739(9)	2.840(3), 2.876(3)	2.632(6), 2.823(6)	2.5116(12)
N(H)---F	2.4367(13), 2.4376(13)	2.937(5), 2.937(5)	2.404(4)	2.5308(17), 2.5396(17)
$F_{ax}{-}S{-}F_{ax}$	176.49(4), 177.23(4)	171.21(18), 170.90(19)	172.06(6)	170.94(7)
$F_{eq}{-}S{-}F_{eq}$	98.49(5), 98.69(6)	99.71(17), 99.47(18)	97.80(7)	97.39(7)

	$[HNC_5H_4N(CH_3)_2^+][HF_2^-]\cdot 2SF_4$	$[HNH_4C_5{-}C_5H_4NH^{2+}]2F^-\cdot 2SF_4$	$[HNH_4C_5{-}C_5H_4N^+]F^-\cdot 4SF_4$
$S{-}F_{eq}$	1.5330(15) to 1.5461(14)	1.510(2), 1.559(2)	1.512(3), 1.547(2)
$S{-}F_{ax}$	1.6326(15) to 1.6825(16)	1.633(2), 1.651(2)	1.642(3), 1.653(2)
S---F	2.6783(18) to 2.8702(18)	2.562(3)	2.658(2), 2.838(3)
N(H)---F	2.633(2), 2.638(2)	2.429(3)	2.427(3)
$F_{ax}{-}S{-}F_{ax}$	170.69(8) to 171.85(7)	173.90(14), 174.25(15)	172.39(11), 174.23(16)
$F_{eq}{-}S{-}F_{eq}$	98.80(8) to 99.24(9)	96.06(11), 98.75(14)	99.83(16), 97.97(13)

The fluoride anions are hydrogen-bonded to pyridinium cations, which are located on alternating sides along the [---S---F---]$_n$ chain. Sulfur tetrafluoride adopts the expected seesaw geometry and has two long contacts (2.6826(9) and 2.7739(9) Å) to the bridging fluorides, which are shorter than the S---F contacts found in solid SF_4 (≥ 2.945(5) Å).[11] The S–F bond lengths (F_{eq}: 1.5398(9) and 1.5425(9) Å; F_{ax}: 1.6622(11) and 1.6680(11) Å) lie in the range found for solid SF_4 (F_{eq}: 1.474(6) to 1.553(4) Å; F_{ax}: 1.635(4) to 1.676(5) Å),[11] reflecting the weakness of the S---F^- interactions. The lone pair bisects the F---S---F contact angle, widening it to 104.35(3)°. The N1(H)---F9 distance (2.4367(13) Å) in $[HNC_5H_5^+]F^-\cdot SF_4$ agrees well with that of $C_5H_5N\cdot HF$ (2.472 Å).[12]

The $[HNC_5H_5^+][HF_2^-]\cdot 2SF_4$ salt also forms a chain structure in the solid state. The structure consists of a double chain composed of alternating SF_4 molecules and HF_2^- ions, where each of the two fluorine atoms of an HF_2^- anion bridge two separate SF_4 molecules. The pyridinium cations hydrogen-bond to the bifluoride anions on both sides of the double chain (Figure 2). The orientation of the SF_4 molecules alternate with the equatorial fluorines pointing below or above the plane formed by the HF_2^- anions.

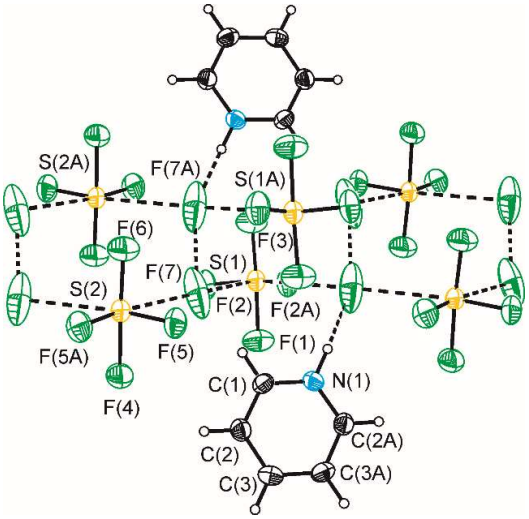

Figure 2. Thermal ellipsoid plot of the $[HNC_5H_5^+][HF_2^-]\cdot 2SF_4$ double chain. Thermal ellipsoids are at 50% probability. The C(1) and N(1) atoms of the pyridinium cation exhibit a symmetry-imposed disorder. The H atom of HF_2^- (F(7)---F(7A)) could not be located in the difference map and is, therefore, not shown.

The pyridinium cation exhibits an orientational disorder. This disorder is imposed by a crystallographic mirror plane, resulting in a disorder of the hydrogen-bond to two bifluoride anions. Depending which side of the HF_2^- anion the pyridinium is hydrogen-bonded to, HF_2^- is expected to be differently polarized, i.e., the hydrogen in HF_2^- will be closer to one or the other fluorine atom (F1−H---F2---$HNC_5H_5^+$ versus $NC_5H_5H^+$---F1---H−F2). As the consequence of these two superimposed structures, the hydrogen in the bifluoride anion is disordered over two positions and could not be located in the difference map, and the thermal ellipsoids of the fluorines are elongated. The F---F distance in bifluoride is 2.241(7) Å which is shorter than the F---F distance found in pyridinium bifluoride (2.326 Å),[12] or 4-methylpyridinium bifluoride (2.322(4) Å) (vide infra).

The N(H)---F (2.937(5) Å) and the S---F (2.840(3) to 2.876(3) Å) distances are much longer in the bifluoride structure than those found in $[HNC_5H_5^+]F^-\cdot SF_4$ ((N(H)---F = 2.4367(13) Å and S---F = 2.6826(9) and 2.7739(9) Å). This agrees with the much weaker basicity of bifluoride compared to that of fluoride. As expected, the weak S---F contacts do not have a marked effect on the S−F bond lengths compared to neat solid SF_4. In addition, these long contacts reflect the relative instability of the crystals towards loss of SF_4 which was observed when handling the crystals in the cold trough at −80 °C while selecting crystals. The N(H)---F contacts are much longer than those found in pyridinium bifluoride (2.508 Å)[12] and 4-methylpyridinium bifluoride (2.533(4) Å) (*vide infra*), and could be imposed by packing of the disordered pyridinium rings. The F---S---F contact angles alternate from 93.8(1)° (S1), and 108.0(1)° (S2). The small angle occurs between two adjacent bifluorides that exhibit disordered hydrogen-bonds to the same pyridinium cations, while the large angle is observed when the bifluorides are hydrogen-bonded to two different pyridinium cations. The variability of the F---S---F contact angle is in line with the weakness of the S---F contacts in this structure.

4-Methylpyridine-HF-SF_4 System. The compound, $[HNC_5H_4(CH_3)^+]F^-{\cdot}SF_4$, crystallizes in the triclinic space group $P\bar{1}$ and contains discrete dimers that consist of two fluoride anions asymmetrically bridging two SF_4 molecules (S1---F5 = 2.632(6) Å, S1---F5A = 2.823(6) Å) (Figure 3). The fluorides are hydrogen-bonded to 4-methylpyridinium cations. The difference in S---F contact strengths does not result in any measurable difference in the S–F bond lengths that are *trans* to the contacts (S1–F1: 1.544(4) Å; S1–F2: 1.543(4) Å). The packing in the crystal structure is remarkably different from the extended chain structures observed for the pyridine-HF-SF_4 system, which is likely a consequence of the para-methyl group preventing efficient packing of potential chain structures in the solid state.

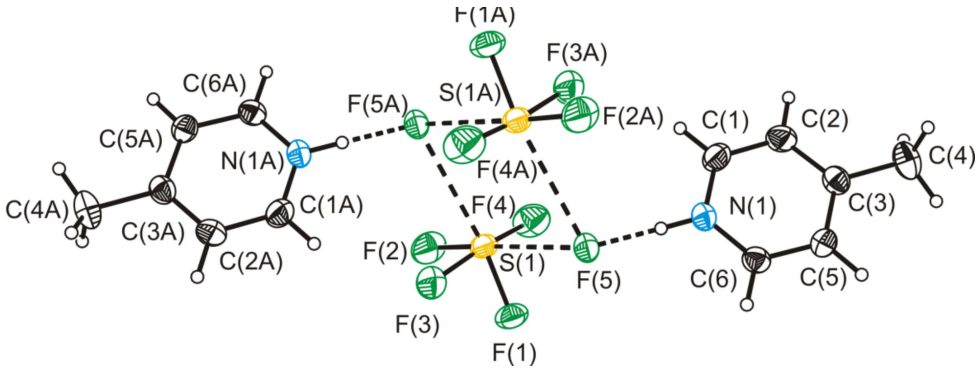

Figure 3. Thermal ellipsoid plot of the dimer present in the crystal structure of $[HNC_5H_4(CH_3)^+]F^-{\bullet}SF_4$. Thermal ellipsoids are at 50% probability.

In the $[HNC_5H_4(CH_3)^+][HF_2^-]$ salt, which crystallized from toluene at low temperature, the 4-methylpyridinium cation is hydrogen-bonded to one of the fluorines of bifluoride (Figure 4). The N1(H)---F1 distance (2.533(4) Å) is longer than the majority of the structures containing fluoride bound to SF_4. The F---F distance in the bifluoride anion (2.323(5) Å) is in excellent agreement with the F---F distance of 2.326 Å found in pyridinium bifluoride.[12] The hydrogen atom was located in the difference map and its position could be refined. As expected, the F1–H distance (1.25(3) Å) is longer than the F2–H distance (1.07(3) Å), due to the hydrogen-bonding interaction between F1 the 4-methylpyridinium cation.

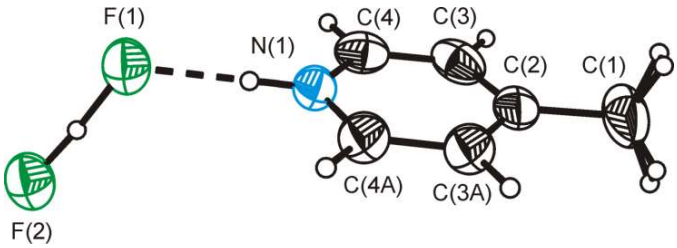

Figure 4. Thermal ellipsoid plot of the $[HNC_5H_4(CH_3)^+]HF_2^-$ ion pair. Thermal ellipsoids are at 50% probability.

2,6-Dimethylpyridine-HF-SF_4 System. The addition of two orthomethyl groups to the pyridine ring prevents hydrogen-bonded fluoride ions to bridge two SF_4 molecules. The resulting structure of $[HNC_5H_3(CH_3)_2^+]_2[SF_5^-]F^-\cdot SF_4$ consists of two 2,6-dimethylpyridinium cations hydrogen-bonded to a single fluoride anion, which is coordinated to a single SF_4 molecule by a relatively strong S---F contact (2.5116(12) Å). The charge of this overall cationic $[HNC_5H_3(CH_3)_2^+]_2F^-$---$SF_4$ moiety is balanced by an isolated SF_5^- anion (see Figure 5).

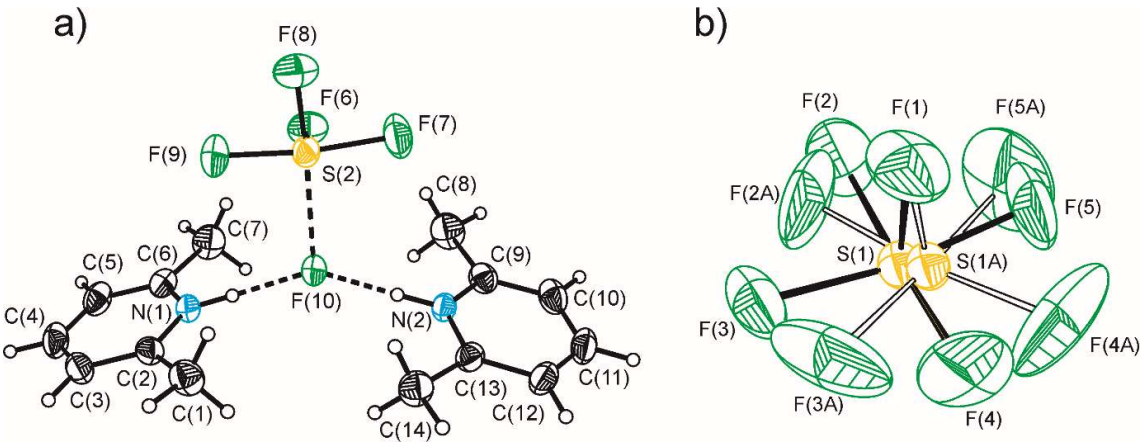

Figure 5. Thermal ellipsoid plot of a) the $[HNC_5H_3(CH_3)_2^+]_2F^-\cdot SF_4$ moiety and b) the disordered SF_5^- anion of $[HNC_5H_3(CH_3)_2^+]_2[SF_5^-]F^-\cdot SF_4$. Thermal ellipsoids are at 50% probability.

The 2,6-dimethylpyridinium cations exhibit long hydrogen bonds to F^- (N1(H)---F10 = 2.5396(17) Å and N2(H)---F10 = 2.5308(17) Å) with an N1(H)---F10---(H)N2 angle of 146.57(6)°. Compared to the structures of $[HNC_5H_5^+]F^-\cdot SF_4$ and $[HNC_5H_4(CH_3)^+]F^-\cdot SF_4$ the

N(H)---F distance in the the dimethylpyridinium structures are longer, reflecting the lower acidity of the 2,6-dimethylpyridinium cation and the fact that two cations are hydrogen-bonded to the same fluoride. The structural motif of the $[HNC_5H_3(CH_3)_2^+]_2F^-$---$SF_4$ moiety is the same as observed in the structure of $[HNC_5H_3(CH_3)_2^+]_2F^-[SF_5^-]\cdot 4SF_4$.[11] The N(H)---F hydrogen bonds in the current structure are somewhat stronger and, as a consequence, the F_4S---F contact is weaker (2.5116(12) Å) in $[HNC_5H_3(CH_3)_2^+]_2[SF_5^-]F^-\bullet SF_4$ versus 2.487(2) Å in $[HNC_5H_3(CH_3)_2^+]_2F^-[SF_5^-]\cdot 4SF_4$).[11] Because of the low Lewis acidity of SF_4, the formation of the SF_5^- anion only occurs with naked fluoride. In $[HNC_5H_3(CH_3)_2^+]_2[SF_5^-]F^-\cdot SF_4$, one fluoride (F10) forms two hydrogen-bonds to two 2,6-dimethylpyridinium cations, rendering the F(10) fluoride not sufficiently 'naked' to yield SF_5^- with SF_4. The second fluoride does not have any H-bonds and can therefore combine with SF_4 to form the SF_5^- anion. The lack of contacts to the SF_5^- anion results in an orientational disorder of this anion, which was modelled with two orientations which have the axial fluorine atom (F1) as the common pivot point. The observed disorder is in contrast to the ordered SF_5^- anion in $[HNC_5H_3(CH_3)_2^+]_2F^-[SF_5^-]\cdot 4SF_4$,[11] which exhibits F_4SF---SF_4 contacts, anchoring the anion into one orientation. The SF_5^- anion adopts the expected square pyramidal structure with a shorter axial S–F bond than the equatorial S–F bonds. The thermal ellipsoids in the equatorial plane are elongated, suggesting some residual rotational motion around the S–F axis.

4-Dimethylaminopyridine-HF-SF_4 System. The structure of $[HNC_5H_4N(CH_3)_2^+][HF_2^-]\cdot 2SF_4$ contains a double chain consisting of bifluoride coordinated to four SF_4 molecules and hydrogen-bonded to one 4-dimethylaminopyridinium cation (Figure 6).

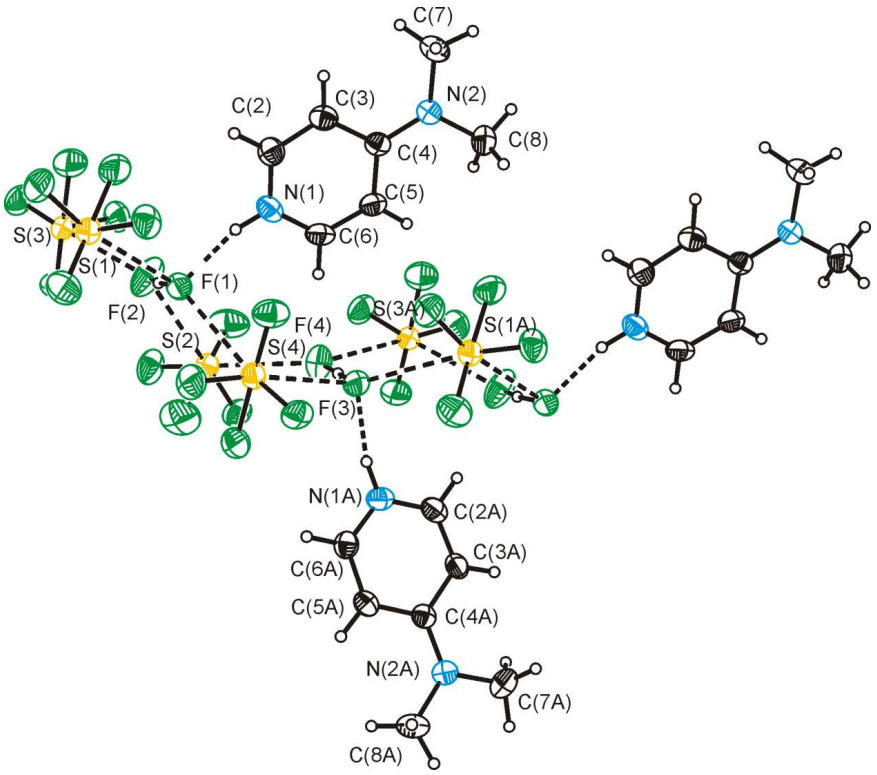

Figure 6. Thermal ellipsoid plot of the $[HNC_5H_4N(CH_3)_2^+][HF_2^-]\cdot 2SF_4$ double chain. Thermal ellipsoids are at 50% probability.

The structural motif is reminiscent of that observed for the $[HNC_5H_5^+][HF_2^-]\cdot 2SF_4$ salt as it contains a double bifluoride-SF_4 chain. The protonated nitrogen-base cations, however, are not disordered, as the dimethylamino group prevents rotation of the pyridinium ring while maintaining the overall packing arrangement. It was therefore possible to locate the hydrogens of the bifluoride anions. The 4-dimethylaminopyridinium cations are all found on one side of the bifluoride chain, which causes polarization of the bifluoride anions. As expected, the fluorides (F1 and F3) that are hydrogen-bonded to the cations have longer F1–H1B/F3–H2B bonds (1.28(3) and 1.25(3) Å) than the F2–H1B/F4–H2B bonds (1.01(3) and 1.05(3) Å). In addition, the thermal ellipsoid of the one fluorine atom of bifluoride, which is hydrogen-bonded to the 4-dimethylaminopyridinium cation, is smaller than that of the other fluorine atom, reflecting the restriction of motion by the hydrogen-bond.

The S---F contacts in this structure have a significant spread (2.678(2) to 2.870(2) Å), with the average of contact distances about each sulfur atom being 2.76/2.77 Å, which is shorter than in the pyridinium bifluoride structure.

The structure of $[HNC_5H_4N(CH_3)_2^+]_2[SF_5^-]F^-\cdot CH_2Cl_2$ consists of two protonated 4-dimethylaminopyridinium cations hydrogen-bonded to a fluoride anion, which in turn has a very weak hydrogen-bond to dichloromethane (see Figure 7).

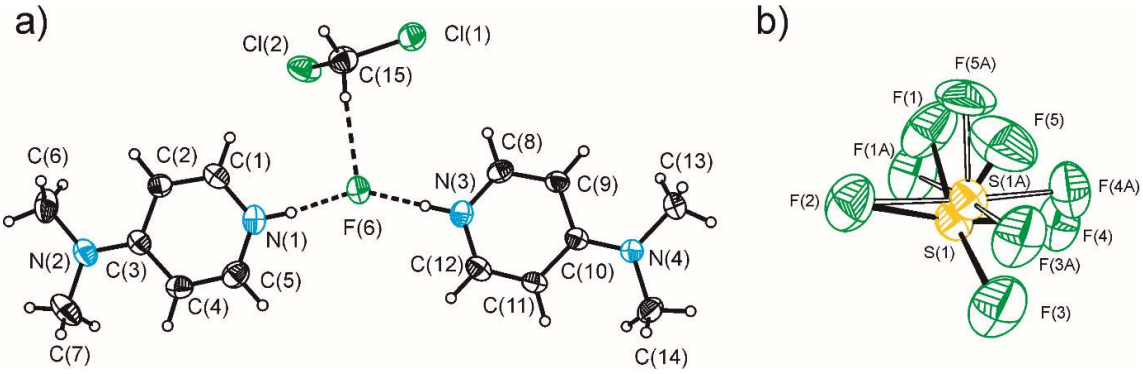

Figure 7. Thermal ellipsoid plot of $[HNC_5H_4N(CH_3)_2^+]_2[SF_5^-]F^-\cdot CH_2Cl_2$. Thermal ellipsoids are at 50% probability.

This structure is similar to that of $[HNC_5H_3(CH_3)_2^+]_2[SF_5^-]F^-\cdot SF_4$ (vide supra), with a dichloromethane molecule in place of the SF_4 molecule coordinated to the fluoride. The very long C(H)---F distance of 3.106(6) Å reflects the weakness of such hydrogen bonds and is longer than the C(H)---F contact (2.969(3) Å) found in the crystal structure of $[C(N(CH_3)_2)_3^+]F^-\cdot CH_2Cl_2$.[13] The charge is balanced by a well separated SF_5^- anion that exhibits a two-fold disorder (Figure 7) with the pivot point being one of the equatorial fluorines, i.e., F(2).

The 4,4'-Bipyridyl-HF-SF_4 System. In the salt of the monoprotonated bipyridinium cation, $[HNH_4C_5{-}C_5H_4N^+]F^-\cdot 2SF_4$, the protonated side of the cation is hydrogen bonded to a fluoride ion, which coordinates to an SF_4 molecule. The non-protonated nitrogen of 4,4-bipyridyl

directly coordinates to an SF_4 molecule (see Figure 8). The S---N contact of 2.614(3) Å is significantly longer than that of $SF_4 \cdot NC_5H_5$ (2.514(2) Å),[4] reflecting the weaker Lewis basicity of the singly protonated 4,4'-bipyridyl ligand compared to pyridine.

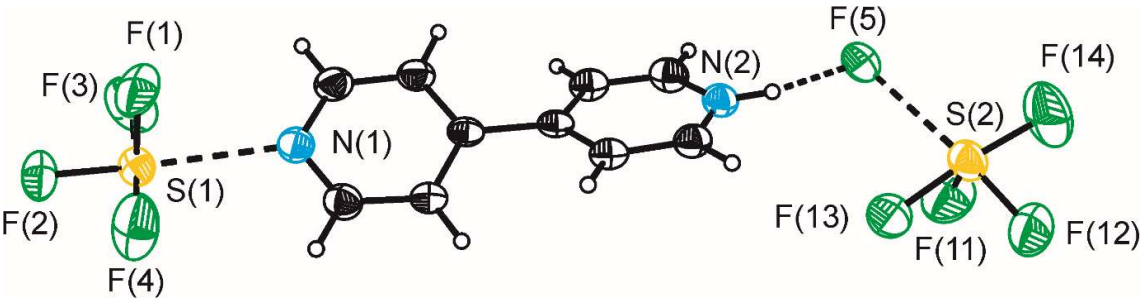

Figure 8. Thermal ellipsoid plot of $[HNH_4C_5{-}C_5H_4N^+]F^- \cdot 2SF_4$. Thermal ellipsoids are at 50% probability.

In the crystal structure of $[HNH_4C_5{-}C_5H_4NH^{2+}]2F^- \cdot 4SF_4$, the two halves of the 4,4'-bipyridyl molecule are related by crystallographic 2-fold rotational symmetry. The two nitrogen atoms of 4,4'-bipyridyl are protonated and the NH groups form hydrogen-bonds to fluoride, which is coordinated to three SF_4 molecules (Figure 9). Two of the three SF_4 molecules are related by crystallographic symmetry. One SF_4 has two comparatively short contacts (2.658(2) and 2.695(3) Å) with two fluorides, forming (---SF_4---F---) chains along the *c*-axis. The second crystallographically unique SF_4 molecule has a long contact (2.838(3) Å) with fluoride.

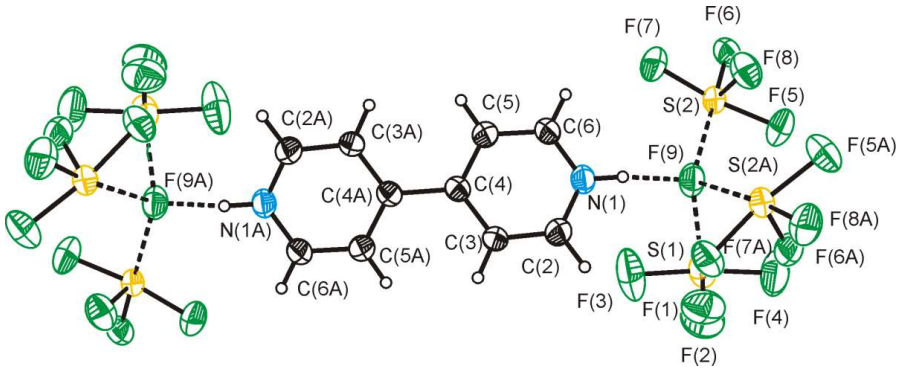

Figure 9. Thermal ellipsoid plot of $[HNH_4C_5{-}C_5H_4NH^{2+}]2F^- \cdot 4SF_4$ with thermal ellipsoids set at 50% probability.

Raman Spectroscopy

Because of the thermal instability of the salts in the present study towards loss of SF_4, low-temperature Raman spectroscopy was used for the characterization of the solid samples, in addition to X-ray crystallography. The Raman bands attributable to the protonated nitrogen bases and the SF_4 groups were assigned based on the Raman spectra of pure SF_4 and those of SF_4 adducts of nitrogen bases.[4] Raman bands of the 4,4'-bipyridyl moiety were assigned based on vibrational assignment of neat 4,4'-bipyridyl.[14]

The low-temperature Raman spectra of $[HNC_5H_5^+][HF_2^-]\cdot 2SF_4$, $[HNC_5H_3(CH_3)_2^+]_2[SF_5^-]F^-\cdot SF_4$, and $[HNC_5H_4N(CH_3)_2^+][HF_2^-]\cdot 2SF_4$ contained signals attributable to the protonated nitrogen bases, as well as weakly coordinated SF_4. No signals arising from the SF_4•*N*-base adducts, free SF_4 and free *N*-base were observed, indicating complete solvolysis of the adducts. For $[HNC_5H_5^+][HF_2^-]\cdot 2SF_4$ and $[HNC_5H_4N(CH_3)_2^+][HF_2^-]\cdot 2SF_4$, bands assigned to the symmetric stretching vibration of HF_2^- were observed at 606 and 609 cm^{-1}. The Raman spectrum of $[HNC_5H_4(CH_3)^+]F^-\cdot SF_4$ still contained bands attributable to the $SF_4\cdot NC_5H_4(CH_3)$ adduct, even after a 1.5-fold excess of HF was used; no signals for HF_2^- were observed in Raman spectra of the solvolysis products of $SF_4\cdot NC_5H_4(CH_3)$.

Selected vibrational frequencies associated with the SF_4 moieties are given in Table 3, while the Raman spectra and complete lists of vibrational frequencies and tentative assignments are given in the Supporting Information (Figures S1 to S4; Tables S10 to S13). In general, the signals attributable to S–F stretching within SF_4 are shifted to lower frequencies from those of neat SF_4, but less than the shifts of SF_4 stretching bands observed for the nitrogen-base-SF_4 adducts.[3,4] This reflects the relatively weak donor properties of hydrogen-bonded fluoride and

Table 3. Selected vibrational frequencies (cm^{-1}) for the SF_4 moieties in $[HNC_5H_5^+][HF_2^-]\cdot 2SF_4$, $[HNC_5H_4(CH_3)^+]F^-\cdot SF_4$, $[HNC_5H_3(CH_3)_2^+]_2[SF_5^-]F^-\cdot SF_4$, $[HNC_5H_4N(CH_3)_2^+][HF_2^-]\cdot 2SF_4$, $[HNH_4C_5{-}C_5H_4NH^{2+}]2F^-\cdot 2SF_4$, and $[HNH_4C_5{-}C_5H_4N^+]F^-\cdot 4SF_4$.

	$[HNC_5H_5^+]$ $[HF_2^-]\cdot 2SF_4$	$[HNC_5H_4(CH_3)^+]$ $F^-\cdot SF_4$	$[HNC_5H_3(CH_3)_2^+]_2$ $[SF_5^-]F^-\cdot SF_4$	$[HNC_5H_4N(CH_3)_2^+]$ $[HF_2^-]\cdot 2SF_4$	$[HNH_4C_5{-}C_5H_4NH^{2+}]$ $2F^-\cdot 2SF_4$	$[HNH_4C_5{-}C_5H_4N^+]F^-\cdot 4SF_4$
$\nu_s(SF_{2eq})$	881(58)	878(100)	859(39)	897(19)/878(23)	897(37)/871(3)	893(42)/880(29) 865(2)/856(8) F_4S---N
$\nu_{as}(SF_{2eq})$	844(23)	828(30)	807(18)	868(23)	862(3)/836(15)	834(3) 824(3) F_4S---N
$\nu_s(SF_{2ax})$	532(58)	530(61)[a]	534(47)	540(34)	533(42)	534(100) 504(21) F_4S---N
$\tau(SF_2)$	454(7)	453(9)/449(6)	441(27)[b]	n.o.	446(6)	452(11) 445(8) F_4S---N
$\delta_{sc}(SF_{2eq}) - \delta_{sc}(SF_{2ax})$	246(3)	261(2)/249(2)	n.o.	248(6)	n.o.	239(12) 276(4) F_4S---N

[a] Overlap an SF_4·N-base adduct signal. [b] Overlap with a band arising from the SF_5^- anion.

bifluoride compared to the relatively strong donor properties of pyridine and its derivatives, as well as triethylamine. As a consequence of the stronger fluorobasicity of F^- compared to HF_2^-, the shifts in SF_4 modes of $[HNC_5H_4(CH_3)^+]F^-\cdot SF_4$ and $[HNC_5H_3(CH_3)_2^+]_2[SF_5^-]F^-\cdot SF_4$ were more substantial than those for the two HF_2^- salts. In the Raman spectrum of $[HNC_5H_4(CH_3)^+]F^-\cdot SF_4$, a number of bands exhibit splittings that can be interpreted with respect to the dimeric solid-state structure.

Raman spectroscopic characterization of $[HNC_5H_5^+]F^-\cdot SF_4$ and $[HNC_5H_4(CH_3)^+][HF_2^-]$ were inconclusive because of the intense signals of toluene, surrounding the crystallized samples, which completely dominated the spectrum and could not be easily removed without loss of SF_4 from the salts.

The Raman spectrum of the $[HNC_5H_4N(CH_3)_2^+]_2[SF_5^-]F^-\cdot CH_2Cl_2$ salt (Figure S5, Table S14) contains signals that can be assigned to CH_2Cl_2, SF_5^-, and the 4-dimethylaminopyridinium cation, as well as signals associated with the SF_4•4-dimethylaminopyridine adduct. The intense band at 697 cm^{-1} is assigned to the $\nu_s(CCl_2)$ mode of dichloromethane and is not significantly shifted relative to neat CH_2Cl_2 (701 cm^{-1}). The SF_5^- anions in $[HNC_5H_4N(CH_3)_2^+]_2[SF_5^-]F^-\cdot CH_2Cl_2$ and $[HNC_5H_3(CH_3)_2^+]_2[SF_5^-]F^-\cdot SF_4$ gave rise to sets of Raman bands, whose assignments are based on those by Thrasher et al.[10] In agreement with previous reports, the S–F_{ax} stretching/ asymmetric equatorial SF_4 stretching bands appear at 796/609 and 790/573 cm^{-1} for $[HNC_5H_4N(CH_3)_2^+]_2[SF_5^-]F^-\cdot CH_2Cl_2$ and $[HNC_5H_3(CH_3)_2^+]_2[SF_5^-]F^-\cdot SF_4$, respectively. The assignments of the strong anion bands between 419 and 441 cm^{-1} is tentative, since three vibrations were predicted to have similar frequencies in this range.[10]

The low-temperature Raman spectrum of $[HNH_4C_5–C_5H_4N^+]F^-\cdot 2SF_4$ (Figure S6, Table S15) includes bands arising from SF_4 that is coordinated to one nitrogen of 4,4'-bipyridyl with S–F stretching frequencies similar to those of the previously reported $SF_4\cdot$*N*-base adducts,[4] as

well as bands attributable to SF_4 that is more weakly coordinated by fluoride. In the Raman spectrum of the sample with the doubly protonated 4,4'-bipyridyl, $[HNH_4C_5{-}C_5H_4NH^{2+}]2F^{-}{\cdot}4SF_4$, (Figure S6, Table S16) the low-frequency S–F stretches attributed to SF_4 adducted to a nitrogen-base are absent and only bands of SF_4 coordinated to F^- were observed.

Conclusion

A range of pyridinium and substituted pyridinium fluoride salts that incorporate sulfur tetrafluoride have been synthesized and characterized by X-ray crystallography and Raman spectroscopy at low temperatures. These structures exhibit a surprising range of structural motifs and provide an extensive view of SF_4 in the solid state and its Lewis acid behavior. The structures offer insights in $F_4S{-}{-}{-}F^-$ interactions, where F^- is not 'naked', which is in contrast to the known $F_4S{-}F^-$ bonds in the SF_5^- anion. In contrast to the S---N in SF_4 nitrogen-base adducts and $S{-}F^-$ bond in SF_5^-, where sulfur interacts with only one Lewis basic group, most structures in the current study show the interaction of sulfur with two Lewis basic fluorine atoms. This is in line with the finding of two σ-holes about sulfur in SF_4.[15] These σ-holes, positive regions on the molecular electrostatic potential, are both opposite of the equatorial S–F bonds and interact with Lewis basic fluorides. The $S{-}{-}{-}F^-$ contacts range from 2.5116(12) to 2.8241(9) Å and are all significantly shorter than the sum of the van-der-Waals radii (3.27 Å). Whereas the bonding in the SF_5^- anion (1.586(2) to 1.718(5) Å) is strongly covalent, the S–F distance is much longer when one fluoride ion that accepts a strong hydrogen bond from a protonated N-base coordinates to SF_4 (2.5116(12) and 2.562(3)Å for $F_4S{-}{-}{-}F^-$ coordination). In such a $F_4S{-}{-}{-}F^-$ coordination, a square-pyramidal geometry about sulfur is maintained. If the coordination environment is extended by a second fluoride, the S–F distance increases further (2.632(6) to 2.838(3) Å for $F_4S({-}{-}{-}F)_2^-$ coordination and 2.683(18) to 2.876(3) Å for $F_4S({-}{-}{-}$

$FHF)_2^-$ coordination) and a distorted octahedral geometry results. The bifluoride anion formed in three of two reaction systems and the F---F distances agree well with previously reported F---F distances of bifluoride. The $[HNC_5H_5^+][HF_2^-]\cdot 2SF_4$ and $[HNC_5H_4N(CH_3)_2^+][HF_2^-]\cdot 2SF_4$ salts are the first examples of SF_4-bifluoride interactions in the solid state. The SF_5^- anion was found in the crystal structures of $[HNC_5H_4N(CH_3)_2^+]_2[SF_5^-]F^-\cdot CH_2Cl_2$ and $[HNC_5H_3(CH_3)_2^+]_2[SF_5^-]F^-\cdot SF_4$, providing higher-accuracy structural information for this important square-pyramidal main-group anion, compared to the three of the four previously reported structures.[6,10] The $[HNH_4C_5{-}C_5H_4N^+]F^-\cdot 2SF_4$ structure contains both F_4S---N and F_4S---(F)---HN bonding, and is therefore a link between the previously characterized SF_4-nitrogen-base adducts,[3,4] and the nitrogen-base-HF-SF_4 salts.

Experimental Section

Materials and Apparatus. All volatile materials were handled (a) on a Pyrex vacuum line equipped with glass/Teflon J. Young valves and (b) a vacuum line constructed of nickel, stainless steel, and FEP. Non-volatile materials were handled in the dry nitrogen atmosphere of a drybox (Omni Lab, Vacuum Atmospheres). Reaction vessels and NMR sample tubes were fabricated from ¼-in. o.d. and 4-mm o.d. FEP tubing, respectively, and outfitted with Kel-F valves. All reaction vessels and sample tubes were rigorously dried under dynamic vacuum prior to passivation with 1 atm F_2 gas.

All of the nitrogen bases were purchased from Sigma-Aldrich. 4-Dimethylaminopyridine (99%) was dried under vacuum. 2,6-Lutidine (≥ 99%) was used as received. 4-Methylpyridine (99%) was purified by freeze-pump-thaw degassing, followed by distilling onto freshly cut potassium, followed by distillation onto dry 4Å-molecular sieves. Pyridine was dried from 4Å molecular sieves and calcium hydride. Sulfur tetrafluoride (Ozark-Mahoning Co.) was purified by passing the gas through an FEP U-trap containing activated

charcoal. Traces of thionyl fluoride and sulfur hexafluoride were present in the sulfur tetrafluoride, but did not interfere with the chemistry.

CAUTION: Sulfur tetrafluoride is a highly toxic and corrosive gas, which easily hydrolyzes to HF. Exposure to these chemicals can cause serious injuries.

Preparation of $[HNC_5H_5^+]F^-{\cdot}SF_4$. Pyridine (0.014 g, 0.18 mmol) was distilled into a ¼-in. FEP reactor. Sulfur tetrafluoride (0.057 g, 0.52 mmol) was vacuum distilled into the reactor at −196 °C. The reactor was warmed to −80 °C and agitated to form a clear colourless solution. Excess SF_4 was removed by pumping at −75 °C for 2 hours, yielding colourless solid $SF_4{\cdot}NC_5H_5$. Approximately 0.05 mL of toluene, which had been apparently insufficiently dried over molecular sieves, was vacuum distilled into the reactor at −196 °C. The reactor was warmed to −60 °C; gas evolution was observed as the adduct dissolved. Large colourless crystalline needles formed overnight at −80 °C.

Preparation of $[HNC_5H_5^+][HF_2^-]{\cdot}2SF_4$. Water (0.013 g, 0.72 mmol) was micro-syringed into a ¼-in. FEP reactor, followed by vacuum distillation of pyridine (0.109 g, 1.38 mmol) at −196 °C. A large excess of SF_4 (ca. 0. 4 g, 4 mmol) was distilled at −196 °C. The reactor was warmed slightly to the melting point of SF_4, and the vigorous reaction was quenched by cooling in liquid nitrogen to control the reaction rate. After no further reaction was observed, the reactor was allowed to warm to room temperature, resulting in a clear colourless solution. Slow cooling to −90 °C resulted in crystal formation. Excess SF_4 and SOF_2 were pumped off at −90 °C.

Preparation of $[HNC_5H_4(CH_3)^+]F^-{\cdot}SF_4$. Water (0.019 g, 1.05 mmol) was micro-syringed into a ¼-in FEP reactor. After vacuum distillation of 4-methylpyridine (0.185 g, 1.99 mmol), SF_4 (0.65 g, 6.4 mmol) was transferred *in vacuo* at −196 °C onto the H_2O and 4-methylpyridine. The reactor was warmed to the melting point of SF_4, and quenched by cooling in liquid nitrogen to control the reaction rate. After no further reaction was observed, the reactor was warmed to room temperature resulting in a clear colourless solution. Slow cooling to −20 °C resulted in

crystal formation. Excess SF_4 and SOF_2 were pumped off at −90 °C, yielding a colourless crystalline solid. The use of 0.006 g (0.3 mmol) water and 0.038 g (0.41 mmol) 4-methylpyridine in excess SF_4 (0.311 g, 2.88 mmol), corresponding to an HF to 4-methylpyridine ratio of 1.5:1 gave, after removal of volatiles at −70 °C, a white powder that was identified by Raman spectroscopy as $[HNC_5H_4(CH_3)^+]F^-\cdot SF_4$ with a small $SF_4\cdot NC_5H_4(CH_3)$ impurity.

Preparation of $[HNC_5H_3(CH_3)_2^+]_2[SF_5^-]F^-\cdot SF_4$. Method 1: After 2,6-dimethylpyridine (0.047 g, 0.44 mmol) was syringed into a ¼-in. FEP reactor, excess sulfur tetrafluoride (ca. 1 g, 9 mmol) was distilled at −196 °C. The reactor was warmed to −80 °C and the reactants mixed. The mixture was placed under dynamic vacuum at −85 °C until a 1:1 mole ratio of SF_4 : 2,6-dimethylpyridine was obtained. Approximately 0.05 mL of toluene containing traces of water was distilled onto the adduct at −196 °C. Upon melting of the toluene, the adduct dissolved and gas evolution was observed. Large plate-like crystals were obtained by cooling from −60 to −80 °C.

Method 2: Water (0.005 g, 0.3 mmol) was micro-syringed into a ¼-in. FEP reactor followed by syringing of 2,6-dimethylpyridine (0.086 g, 0.80 mmol) into the reactor. Subsequently, SF_4 (0.375 g, 3.47 mmol) was vacuum distilled at −196 °C onto the frozen solid. The mixture was warmed slightly and liquid nitrogen was used to quench the vigorous reaction. The reaction mixture was warmed to −45 °C and mixed, resulting in a clear colourless solution. Slow cooling to −85 °C resulted in growth of clear colourless crystals. Excess SF_4 and SOF_2 were removed at −90 °C under dynamic vacuum.

Preparation of $[HNC_5H_4N(CH_3)_2^+][HF_2^-]\cdot 2SF_4$. Inside a dry box, 4-dimethylaminopyridine (0.026 g, 0.21 mmol) was transferred to a ¼-in. FEP reactor. Water (0.002 g, 0.1 mmol) was micro-syringed into the reactor, followed by distillation of an excess of SF_4 (ca. 0.04 mL, 0.7 mmol) at −196 °C. The reactor was slowly warmed to 3 °C, resulting

in a clear colourless solution. Slow cooling to −20 °C resulted in the formation of large needles. Further cooling to −40 °C caused the crystals to grow considerably. Excess SF_4 and SOF_2 were removed between −97 and −87 °C, which caused precipitation of a white powder.

Preparation of $[HNC_5H_4N(CH_3)_2^+]_2[SF_5^-]F^-\cdot CH_2Cl_2$. Inside a dry box, 4-dimethylaminopyridine (0.023 g, 0.19 mmol) was transferred to a ¼-in. FEP reactor. A large excess of SF_4 (ca. 0.04 mL, 0.7 mmol) was vacuum distilled at −196 °C onto the 4-dimethylaminopyridine, and the reactor was stored at −70 °C in a cryo-bath. Approximately 0.05 mL of CH_2Cl_2, which apparently contained moisture, was distilled onto the mixture and the reactor was agitated and warmed to −60 °C, resulting in a clear colourless solution. Removal of volatiles under dynamic vacuum at −80 °C resulted in large needles, with a small amount of yellow powder.

Preparation of $[HNH_4C_5{-}C_5H_4N^+]F^-\cdot 2SF_4$. Inside a dry box 4,4'-bipyridyl (0.022 g, 0.14 mmol) was added to a ¼-in. FEP reactor. Water (0.001 g, 0.06 mmol) was micro-syringed into the reactor. A large excess of SF_4 (ca. 0.04 mL, 0.7 mmol) was distilled at −196 °C. The reactor was warmed to −80 °C which caused the brown solid 4,4'-bipyridyl to turn colourless. Further warming resulted in a clear pale yellow solution. Slow cooling resulted in growth of large needles. Volatiles were pumped off at −70 °C.

Preparation of $[HNH_4C_5{-}C_5H_4NH^{2+}]2F^-\cdot 4SF_4$. Inside a dry box, 4,4'-bipyridyl (0.009 g, 0.06 mmol) was added to a ¼-in. FEP reactor. Water (0.001 g, 0.06 mmol) was micro-syringed into the reactor. A large excess of SF_4 (ca. 0.1 mL) was distilled at −196 °C. Subsequent warming of the reactor to room temperature caused a portion of the colourless solid to dissolve, but the solubility was relatively low. Slow cooling to −80 °C, resulted in the formation of large needles. Excess SF_4 and SOF_2 were pumped off at −90 °C.

Preparation of $[HNC_5H_4(CH_3)^+]HF_2^-$. After distillation of 4-methylpyridine (0.073 g, 0.78 mmol) into a ¼-in. FEP reactor, SF_4 (0.23 g, 2.1 mmol) was transferred *in vacuo* onto

the frozen solid. A slow reaction proceeded at −80 °C, dissolving the solid yielding a clear colourless solution. Volatiles were removed at −75 °C. The reactor only contained 0.4 mmol of SF_4 after removal of volatiles. The reactor was warmed to room temperature, causing the solid to melt and form a colourless yellow liquid. Toluene, containing traces of H_2O, was distilled onto the solid at −196 °C. While the solid dissolved, gas evolved at −60 °C. The reactor was heat-sealed under vacuum and stored in the cryo-bath at −80 °C. Large needles formed, which, when mounted on the diffractometer, had very weak reflections.

Raman spectroscopy. All Raman spectra were recorded on a Bruker RFS 100 FT Raman spectrometer with a quartz beam splitter, a liquid-nitrogen cooled Ge detector, and R-496 temperature accessory. The actual usable Stokes range was 50 to 3500 cm^{-1}. The 1064-nm line of an Nd:YAG laser was used for excitation of the sample. The Raman spectra were recorded with a spectral resolution of 2 cm^{-1} using laser powers of 150 mW.

X-ray crystallography: Crystals were mounted at low temperature under a stream of dry cold nitrogen as previously described.[16] For wet samples, cut FEP tubes were manipulated in the cold trough, at temperatures just above the freezing point of the solvent. Solvents were removed using a combination of glass pipettes and capillary action of Kimwipes®. For extra sensitive crystals, the crystals were removed with the tip of a glass pipette and were directly affixed onto either a glass fiber, or a nylon cryo-loop dipped in inert perfluorinated polyethers, Fomblin Z-25 or Z-15 (Ausimont Inc.). The use of a round FEP tray, inside the trough, was also used to manipulate crystals which decomposed on contact with the metal troughs. The crystals were centered on a Bruker SMART APEX II diffractometer, controlled by the APEX2 Graphical User Interfact software.[17] The program SADABS[18] was used for scaling of diffraction data, the application of a decay correction, and a multi-scan absorption correction. Program SHELXS-97 (Sheldrick, 2008)[19] was used for both solution and refinement. Structure solutions were obtained by direct methods. CCDC 1477903 to 1477911 contain the

crystallographic data. These data can be obtained free of charge from The Cambridge Crystallographic Data Centre via www.ccdc.cam.ac.uk/data_request/cif.

Acknowledgements

We thank the Natural Sciences and Engineering Research Council of Canada (NSERC), the Canadian Foundation for Innovation (CFI), and the University of Lethbridge for funding.

References

(1) Dmowski, W. Introduction of Fluorine Using Sulfur Tetrafluoride and Analogs, In Organo-Fluorine Compounds, Methods of Organic Chemistry; Baasner, B.; Hagemann, H.; Tatlow, J. C.; Eds.; Houben-Weyl, Vol. E10a, Thieme, Stuttgart, 2000, ch. 8, pp. 321-431.

(2) Goettel, J. T.; Turnbull, D.; Gerken, M. *J. Fluorine Chem.* **2015**, *174*, 8-13.

(3) Goettel, J. T.; Chaudhary, P.; Mercier, H. P. A.; Hazendonk, P.; Gerken, M. *Chem. Commun.* **2012**, *48*, 9120-9122.

(4) Chaudhary, P.; Goettel, J. T.; Mercier, H. P. A.; Sowlat-Hashjin, S.; Hazendonk, P.; Gerken, M. *Chem. Eur. J.* **2015**, *21*, 6247-6256.

(5) Tunder, R.; Siegel, B. *J. Inorg. Nucl. Chem.* **1963**, *25*, 1097-1098.

(6) Bittner, J.; Fuchs, J.; Seppelt, K. *Z. Anorg. Allg. Chem.* **1988**, *557*, 182-190.

(7) Drullinger, L. F.; Griffths, J. E. *Spectrochim. Acta A* **1971**, *27*, 1793-1799.

(8) Christe, K. O.; Curtis, E. C.; Schack, C. J.; Pilipovich, D. *Inorg. Chem.* **1972**, *11*, 1679-1682.

(9) Heilemann, W.; Mews, R.; Pohl, S.; Saak, W. *Chem. Ber.* **1989**, *122*, 427-432.

(10) Clark, M.; Kellen-Yuen, C.; Robinson, K.; Zhang, H.; Yang, Z.-Y.; Madappat, K.; Fuller, J.; Atwood, J.; Thrasher, J. *Eur. J. Solid State Inorg. Chem.* **1992**, *29*, 809-833.

(11) Goettel, J. T.; Kostiuk, N.; Gerken, M. *Angew. Chem. Int. Ed.* **2013**, *52*, 8037-8040.

(12) Boenigk, D.; Mootz, D. *J. Am. Chem. Soc.* **1988**, *110*, 2135-2139.

(13) Kolomeitsev, A. A.; Bissky, G.; Barten, J.; Kalinovich, N.; Lork, E.; Röschenthaler, G. V. *Inorg. Chem* **2002**, *41*, 6118-6124.

(14) Topaçli, A.; Akyüz, S. *Spectrochim. Acta, Part A* **1995**, *51*, 633-641.

(15) Nziko, V. d. P. N., Scheiner, S. *J. Phys. Chem.* **2014**, *118*, 10849-10856.

(16) Gerken, M.; Dixon, D. A.; Schrobilgen, G. J. *Inorg. Chem.* **2000**, *39*, 4244-4255.

(17) *APEX* 2, Version 2.2-0; Bruker AXS Inc.: Madison, WI, **2007**.

(18) Sheldrick, G. M. *SADABS*, Version 2007/4, Bruker ACS Inc.; Madison, WI, **2007**.

(19) Sheldrick, G. M. *SHELXTL97*, University of Göttingen, Germany, **2007**.

Table of Contents Graphic and Caption

Adducts between SF_4 and nitrogen-bases are readily solvolysed by HF, yielding the protonated base and fluoride. In the solid state, weakly Lewis acidic SF_4 exhibits different interaction modalities with fluoride.